H_∞ Optimal Controller Design and Reduction for the Inertial Hold Mode of the Attitude Control System of the XTE Spacecraft

(Technical Report to NASA)

P. I. Zhong Ling Xu

R. A. Gui An Zhou

Mathematics Departmant
The University of Texas at Brownsville
80 Fort Brown/Brownsville, Texas 78520

February 5, 1994

H_∞ Optimal Controller Design and Reduction for the Inertial Hold Mode of the Attitude Control System of the XTE Spacecraft

Abstract

The Inertial Hold Mode (IHM) is one mode of the attitude control system of the X-ray Timing Explorer spacecraft disturbed by both parametric uncertainties and external torque disturbance. In the paper, the IHM model is modified into a typical H_∞ mixed-sensitivity problem through choosing suitable weighting functions $W_1(s)$ and $W_3(s)$. The controller is designed by the H_∞ optimization technique with the transformation of shifting the imaginary axis. It can stabilize the plant with uncertainties from the natural frequencies of the flexible body and the very weak damping and provide adequate disturbance rejection as a good regulator. The gain margin and phase margin of the system are 24.03 db and 55.04°, respectively. The step response attenuates to zero within 150 seconds. These show that the controller satisfies the specified requirements. Since the order of the controller appears high, it is reduced to fourth order one. The results show that the stability and the performance of the system with the reduced controller are retained perfectly.

1. Introduction

Inertial Hold Mode (IHM), one mode of the Attitude Control System (ACS), provides inertial pointing to support the X-ray Timing Explorer spacecraft's science operations. In the inertial attitude acquisition phase, it holds attitude with Kalman filter updates based on observed (non-catalog) guide stars until the ground completes an attitude quaternion to the ACS.

IHM holds the correct attitude reference constant, with the exception of small changes to correct for velocity aberration. This allows the High Energy X-ray Timing Experiment and the Proportional Counter Array to make observations and also keeps the spacecraft in a safe attitude with respect to power and thermal requirements [1].

The IHM model mainly consists of plant, gyro, controller and reaction wheel. The transfer function of the flexible body not only has several parallel quadratic transfer functions with a very weak structural damping value of 0.001, but also its natural frequencies of the flexible body may vary +/- 25%. Such light damping may result in harmonic vibration of the spacecraft. It is very dangerous to the spacecraft if the controller can not supply strong rejection on the frequency bandwidth on which the natural frequencies are located.

The problem facing us is to design a controller that will stabilize the plant in the face of

the uncertainties of the variable natural frequencies and the weak damping of the plant model, in other word, the plant will be robust stable under the perturbations of the uncertainties. The controller will satisfies the requirements of the stability margins from the point of view of the classical control theory, such as Gain margin $>$ 12 db and Phase Margin $>$ 30 degree [2]. It must also perform as a good regulator to provide an adequate rejection to the total torque disturbances acting on the spacecraft. In addition, the controller should also be realized easily, its order as low as possible.

The H_∞ technique is a powerful tool to handle control systems with uncertainties and disturbances. It can maximize the level of robust stability and robust performance of the system. By the state-space approach [3,4,5,6] to H_∞ optimization, for which the procedure [7, 8] is automatic and easy to use, a (sub-)optimal controller can be easily obtained. We apply the technique to the controller system.

The order of controller designed by the H_∞ technique is guaranteed to be not higher than that of the generalized plant. However, in many engineering problems, the order of the generalized plant can be very high. This is due to the fact that the generalized plant consists of the original plant as well as all the weighting matrices which are chosen to meet certain design specifications. Hence, the order of the H_∞ controller obtained by the standard state-space approach is usually too high to be implemented in practice, and therefore it is desired to reduced the controller order.

Many approaches have been proposed in the literature in the last decade or so [10 — 13]. However, these reduction approaches are proven to be unsatisfactory and not suitable to our problem because the stability of the system with the reduced controller loses easily. We are trying to find a better controller order reduction method, which will be present in another paper soon.

Two results are presented in this paper. The first is modification of the system into a typical mixed-sensitivity problem by choosing suitable weighting functions $W_1(s)$ and $W_3(s)$, and designing it by the H_∞ optimization technique with the transformation of shifting the imaginary axis. The controller is satisfied to the specified requirements as above.

The second is reduction to the controller since its order is high. In order to retain the stability and the performance of the system, we eliminate the zeros and poles far away from the imaginary axis or the original point so that the frequency characteristics of the reduced controller approaches very closely that of the original ones in the low and middle frequencies bandwidthes. The results are shown below.

IHM is actually a sampled-data model. The continuous-time model however is considered in this paper. According our research schedule, the design of the discrete-time controller will be extended at the next logical step.

2. Modifying IHM into H_∞ Optimization Problem

A right-handed, orthogonal coordinate system — Spacecraft Frame [2] have been defined for XTE as Figure 1.

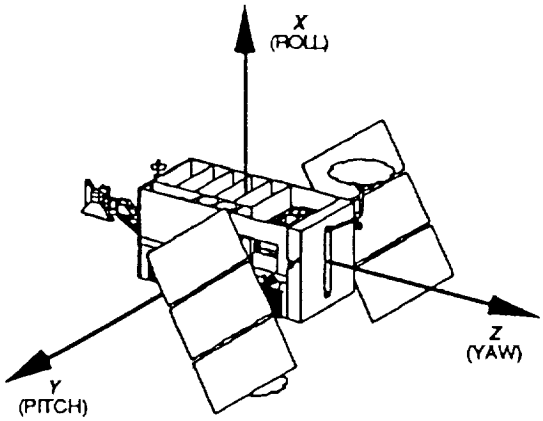

Figure 1. Spacecraft Frame

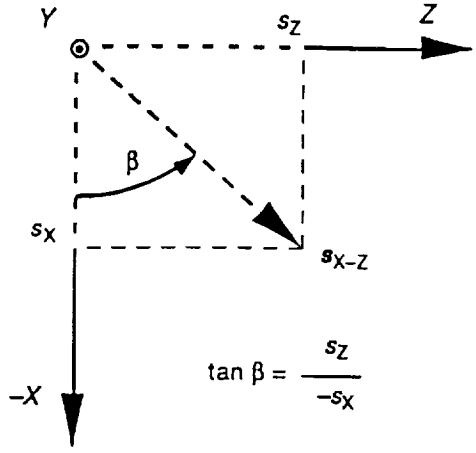

Figure 2. β Angle

The direction of the spacecraft relative to the sun is described in terms of α angle and β angle of the sun vector which is running from the origin of the Spacecraft Frame towards the sun. α is defined in the Y-Z plant. β is defined in the X-Z plant as Figure 2. For different axis and β angle, some parameters in the IHM model are different.

The single axis block diagram of the IHM model mainly consists of plant, gyro, controller and reaction wheel. It is shown below:

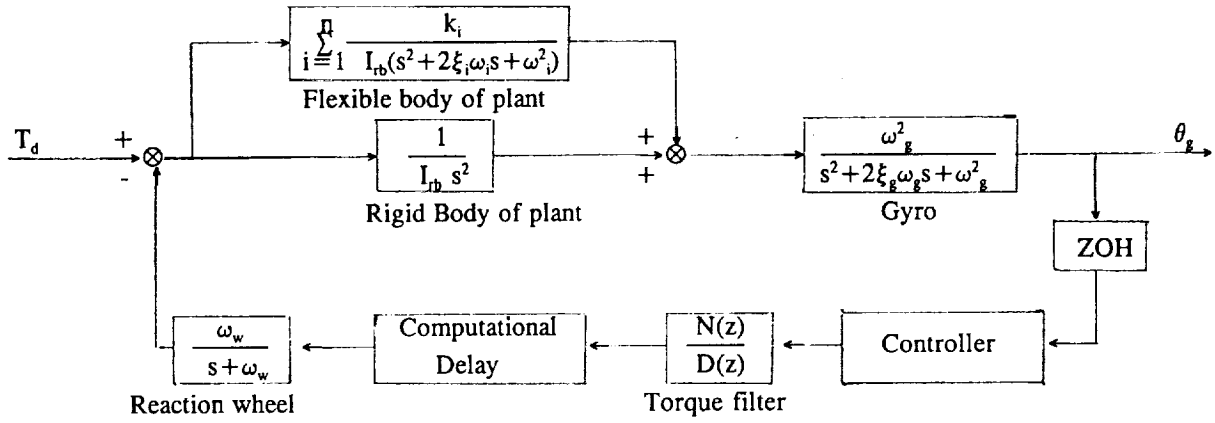

Figure 3. The block diagram of IHM model

The plant has two parts, rigid body and flexible body. The transfer function of the rigid body is simple as follows:

$$G_{rp}(s) = \frac{1}{I_{rb}\, s^2} \tag{2.1}$$

where I_{rb} is the moment of inertia of the rigid body.

The transfer function of the flexible body is much more complicated. It is has several parallel quadratic transfer functions with very weak structural damping value as follows:

$$G_{fp}(s) = \sum_{i=1}^{n} \frac{k_i}{I_{rb}\,(s^2+2\xi_i\omega_i s+\omega^2_i)} \tag{2.2}$$

where k_i is a constant. ω_i is the natural frequencies of the flexible body which locate on the frequency bandwidth of [4.3, 21.3] radian/second. However, these natural frequencies may vary +/-25%. This wide variation will largely extend the locating range of the natural frequencies to [3.3, 26.6] radian/second. ξ_i is the structural damping coefficient with the possible minimum value of 0.001. Such light damping may result in harmonic vibration of the spacecraft. It is very dangerous to the spacecraft if the controller can not supply strong rejection on the extended frequency bandwidth on which the natural frequencies are located.

The values of I_{rb}, k_i and ω_i are different for X, Y or Z axes and β = 0, 45, 90 or 150 degree. They are shown in [2].

The transfer function of the gyro is given by

$$G_g(s) = \frac{\omega^2_g}{s^2+2\xi_g\omega_g s+\omega^2_g} \tag{2.3}$$

where ω_g is the natural frequency of the gyro with value of 2π*7 radian/second and ξ_g is the structural damping coefficient with the value of 0.707.

The transfer function of the reaction wheel is

$$G_w(s) = \frac{\omega_w}{s+\omega_w} \tag{2.4}$$

where ω_w is the constant with the value of 2π*10 radian/second.

Since the controller is a sample-data one in practice, the linear approximation of the sampler and the zero order hold (ZOH) is as

$$G_z(s) = \frac{2}{T_z s+2} \tag{2.5}$$

where T_z is the time constant of sampler-data with the value of 0.25 second.

The linear approximation of the computational delay is

$$G_c(s) = \frac{1}{T_c s+1} \tag{2.6}$$

where T_c is the computational delay with the value of 0.1 second.

The input of the model is T_d which is the total torque disturbance acting on the spacecraft. The output is the gyro model measure θ_g.

The difficulty of designing a controller for IHM mainly comes from the flexible body of the plant. That is, it not only has several parallel quadratic transfer functions with very weak damping, and also its natural frequencies are uncertain. In order to avoid the possible harmonic vibration of the spacecraft, we must design a controller which will have sufficient stability margins and can provide strong rejection to the inner perturbations from the parametric uncertainties and external torque disturbances.

The H_∞ technique is a powerful tool to handle control systems with uncertainties and disturbances. Especially, the H_∞ mixed-sensitivity method is most direct and efficient to single-input and single-output control system. But employing it necessarily requires the parametric uncertainties to be covered by a non-parametric uncertainty model. We model the parametric uncertainty with a single non-parametric block in order to retain the simplicity and intuition of single-loop control.

Without considering of I_{rb}, the transfer functions of the flexible body for all X, Y and Z axes at different directions are shown in Figure 4, which clearly shows that the natural frequencies locate on the bandwidth of [4.3, 21.3] radian/second and the transfer functions of the flexible body of Z axis at $\beta = 0$ degree is almost maximum. To avoid raising the order of the system and to design a controller suitable for all three axes and all directions, we will take the entire flexible body as an additive perturbation of the plant and find a third transfer function as a maximum perturbation rather than a higher order one to cover it.

The non-parametric maximum additive perturbation is given as

$$\Delta_a(s) = \frac{2.3(s+6)}{I_{rb}\,(s+18.8)(s^2+2\xi_a\omega_a s+\omega^2_a)} \tag{2.7}$$

where $\omega_a \approx \omega_1$ because the first natural frequency of the flexible body is most harmful to spacecraft and most needed to be rejected by the H_∞ technique. ξ_a is chosen to 0.1 rather than 0.001 because a too small ξ_a may cause the system unstable.

As Figure 5 shows, the transfer function of the flexible body varying in a shadow with the frequencies ω_i vary by +/- 25%. $\Delta_a(s)$ almost covers the transfer function of the flexible

body except for some peaks. It is justified later that a simpler, unentire cover could be more suitable than a complicated, entire one. The robustness of the controller designed by the H_∞ technique is still guaranteed under such a simplified perturbation cover.

For convenience, the additive perturbation (2.7) is changed into the multiplicative one

$$\Delta_m(s) = \frac{\Delta_a(s)}{G_{rp}(s)} \tag{2.8}$$

where $G_{rp}(s)$ is the transfer function of the rigid body of the plant. $\Delta_m(s)$ is more advantage than $\Delta_a(s)$, because it does not include I_{rb} like $\Delta_a(s)$.

Defining $W_3(s)$ as

$$W_3(s) = e\ \Delta_m(s) \tag{2.9}$$

where $W_3(s)$ is a weighting function affecting robust stability and e is a constant slightly bigger than 1, for example, e=1.05. $W_3(s)$ satisfies

$$\| \Delta_m(j\omega) \|_\infty \leq |W_3(j\omega)| \qquad \forall\omega \tag{2.10}$$

Now we will define another weighting function affecting robust performance, which is denoted by $W_1(s)$. In order to make the system possess adequate disturbance rejection, i.e., the output is as small as possible for the given input. We choose

$$W_1(s) = \frac{14(s+0.05)^2}{s} G_{rp}(s)\ G_g(s) \tag{2.11}$$

where we use $G_p(s)G_g(s)$ because the closed-loop transfer function from torque disturbance to gyro measure output for our system in fact is $G_{rp}(s)G_g(s)(1+GK)^{-1}$, rather than $(1+GK)^{-1}$ as in other mixed-sensitivity problem.

The nominal system is as

$$G(s) = G_{rp}(s)\ G_g(s)\ G_w(s)\ G_z(s)\ G_c(s) \tag{2.12}$$

where $G_{rp}(s)$, $G_g(s)$, $G_w(s)$, $G_z(s)$ and $G_c(s)$ were defined above. The torque filter is ignored in the design. In fact, according to our experience, ignoring the ZOH $G_z(s)$ and the computational delay $G_c(s)$ in design is helpful to increase the robustness of the system because that the controller designed by H_∞ technique will have the zeros with same values as the poles of ZOH and the delay if which are considered, while such zeros will lift the magnitude of the open loop

transfer function of the system on the frequency bandwidth on which the natural frequenies of the flexible body locate. But now the ZOH and the delay are still retained and their influence will be eliminated by reducing the controller in Sector 4.

Let K(s) denote the controller and consider

$$\{\| W_1(1+GK)^{-1} \|_\infty + \| W_3GK(1+GK)^{-1} \|_\infty\} < 1 \qquad (2.13)$$

thus a standard mixed-sensitivity problem is obtained. For the uncertainty bounded by $W_3(s)$ and the disturbance bounded by $W_1(s)$, if there exists a controller K(s) to stabilize the nominal system G(s) and satisfy (2.13), the nominal system will be robust stable. Such an optimal controller is easily designed by the H_∞ technique.

3. H_∞ Controller Design for IHM

Due to some poles of the nominal system G(s) and the weighting function $W_1(s)$ lying on the imaginary axis, the H_∞ optimization algorithm cannot be used directly. By the transformation of shifting the imaginary axis, the controller is designed by the H_∞ optimization procedure [7] as follows.

$$K(s) = \frac{743.75I_{rb}(s+.042\pm.0144i)(s+.47\pm4.79i)(s+8)(s+10)(s+19.13)(s+31.1\pm31.1i)(s+62.83)}{s(s+1.155)(s+5.72)(s+31.24)(s+14.48\pm51.29i)(s+59.46\pm14.60i)(s+40.11\pm41.96i)} \qquad (3.1)$$

The infinity norm of the closed-loop transfer function is shown in Figure 6. The sensitivity function S and the complementary sensitivity function T are shown in Figures 7 and 8, respectively. Figure 8 shown that there exists enough margin for T to $W_3^{-1}(s)$. The robustness of the system is satisfactory for the specified uncertainties covered by $W_3(s)$ and for those peaks not covered by it. It is justified that a simpler unentire cover could be more suitable than a complicated entire one.

The open-loop transfer functions of the system for all three axes at any direction are shown in Figure 9 when taking the controller (3.1) into Figure 1. They are almost entirely the same in low and middle frequency bandwidthes. This implies that they have same stability margins for all three axes at any direction. The stability margins are shown in Figure 10. The minimum gain margin is 24.03 db and the phase margin is 55.04°, which are larger than the expected 12 db and 30°, respectively.

Figure 11 — 13 also show that the variety of the natural frequencies ω_i between -25% and 25% does not greatly affect the open-loop frequency characteristics. This implies that the system is robust stable.

The variation of the natural frequencies of the flexible body or the direction of the spacecraft does not affect the response performance. The unit step responses for three axes are shown in Figure 14 — 16. The responses attenuated to zero for about 150 seconds, which is faster than that of the PID controller [2]. The maximum magnitude of the responses are not higher than that of the PID controller. Our controller performs as a good regulator.

It is worth while to mention here that the larger stability margin could be obtained by adjusting the weighting function $W_1(s)$ and $W_3(s)$, but it would lose a little of the response performance. The choice depends on which is more desirable. We think our choice is moderate.

4. Controller Reduction

A controller with satisfactory robust stability and performance for the spacecraft has been designed. But its order appears high and is difficult to be realized in practice. It should be reduced.

It is well known that the stability and performance of a system is determined by its open-loop frequency characteristic, that is, the product of transfer functions of the controller and generalized plant. If the characteristic is satisfied, our goal is just to find a reduced controller with which the frequency characteristic of the open loop system approaches as close to the original as possible.

Such reduced controllers could be found through eliminating the zeros and poles of the controller (3.1) which are far away from the imaginary axis or the original point. A fourth order reduced controller is given as follows

$$K_4(s) = \frac{23.16I_{tb}(s+.042\pm.0144i)(s+.47\pm4.79i)}{s(s+1.155)(s+5.72)(s+187.44)} \qquad (4.1)$$

The frequency characteristics of the original controller and the reduced one are shown in Figure 17. They are almost entirely the same in low and middle frequency bandwidthes, which implies that the stability and the performance of the system is retained. The magnitudes of the reduced controllers are lower in the frequency bandwidth of [3.3, 26.6] radian/second. It is also helpful to increase the robustness and rejection to the perturbations of the uncertainties of the natural frequencies of the flexible body. We discover that the situation also happens if ignoring ZOH and the delay in the design of the controller (3.1). Sometimes a simpler nominal system may help to design a more robust controller.

The open loop frequency characteristics of the systems with respect to the original controller and to the reduced controller are shown in Figure 18. They are also almost entirely

the same on low and middle frequency bandwidthes and have very similar stability margins. The gain margin and the phase margin reach up to 22.59 db and 54.29 , respectively.

The magnitudes of the open loop frequency characteristics of the systems with respect to the reduced controllers are lower in the frequency bandwidth of [3.3, 26.6] radian/second. This will increase the robustness and rejection of the system to the perturbation of the variation of the natural frequencies of the flexible body.

The unit step response of the closed-loop feedback system for Z axis at $\beta = 0$ degree is shown in Figure 19. It is not greatly different from that of the original controller (3.1).

These results mean the stability and the performance have still been retained perfectly and the reduced controller are satisfactory.

Let us discuss further a second order reduced controller as follows

$$K_2(s) = \frac{3.75I_{rb}(s+.042\pm.0144i)}{s(s+11.55)} \tag{4.2}$$

The open loop frequency characteristics of the systems with respect to the original controller and to the reduced controller are shown in Figure 20. They have slightly difference on low and middle frequency bandwidthes. The system is also stable. As shown in Figure 21, the gain margin and the phase margin reach up to 20.69 db and 66.83, respectively.

But the magnitudes of the open loop frequency characteristics of the systems with respect to the reduced controllers are much higher in the frequency bandwidth of [3.3, 26.6] radian/second. This will lose some robustness and rejection of the system to the perturbation of the variation of the natural frequencies of the flexible body. The situation also happens for the PID controller [2]. As a conclusion, the robustness is not sufficient for a second order controller or a PID controller. A fourth or higher order controller should be adopted for IHM model.

The unit step response of the closed-loop feedback system with the second order reduced controller is shown in Figure 22. It is slight different from that of the original controller (3.1).

5. Conclusions

The IHM model of the attitude control system of the XTE spacecraft with both parametric uncertainties and external torque disturbances is studied in the paper. It is modified into a typical mixed-sensitivity problem by choosing suitable weighting functions $W_1(s)$ and $W_3(s)$. The controller is designed by the H_∞ optimization technique with the transformation of the shifted $j\omega$-axis.

The controller is satisfied entirely to the specified requirements. That is, it can stabilize

the plant in the face of the uncertainties of the natural frequencies and light damping and can provide adequate disturbance rejection.

Since the order of the controller is high, it is reduced by eliminating the zeros and poles far away from the imaginary axis or the original point. The results show that the stability and the robust performance of the system with the fourth order reduced controller are retained perfectly. But a second order reduced controller or a PID controller will lose some robustness.

As the IHM model is actually controlled by computer, the further work is to design a sampler-data controller for it.

References

[1] XTE Attitude Control subsystem analysis document

[2] XTE Attitude Control subsystem analysis document

[3] J.C. Doyle, K. Glover, P.P. Khargonekar, and B.A. Francis, "State-space Solution to Standard H^2 and H^∞ Control Problems," IEEE Transactions on Automatic Control, Vol.AC-34, No.8, 1989.

[4] J.C. Doyle and etc. Feedback Control Theory, Macmillan Publishing Company, New York, 1992.

[5] S. Skogestad, M. Morari and J.C. Doyle, "Robust Control of Ill-Conditional Plants: High-purity Distillation," IEEE Trans. on Auto Control 1988.

[6] M. Morari and E. Zafirion, Robust Process Control, Englewood Cliffs, N.J., Prentice Hall, 1989.

[7] Richard Y. Chiang, Michael G. Safenov, "Robust control Tool Box: User's Guide", The Math Works, Inc., 1992.

[8] G.J. Balas, J.C. Doyle, K. Glover, A. Packard, R. Smith, "μ-Analysis and Synthesis Box: User's Guide", The Math Works, Inc., 1992.

[9] D.P. Lawrance, Issues in Using Non-parametric Models to Represent Parametric Uncertainty, Master's Thesis, University of Massachusetts at Amherst 1991.

[10] B.C. Moore, "Principal Component Analysis in Linear Systems," IEEE Transactions on Automatic Control, Vol.AC-26, No.2, 1981.

[11] K. Glover, "All Optimal Hankel-Norm Approximations of Linear Multivariables Systems and Their L^∞-Error Bounds," Int. J. Control, Vol.39, No.6, 1984

[12] D. Enns, "Model Reduction with Balanced Realizations: An Error Bound and A Frequency Weighted Generalization," Proc. 23rd Conf. Dec. Contr., Las Vagas, NV. 1984.

[13] U.B. Desai and D. Pal, "A Transformation Approach to Stochastic Model Reduction," IEEE Transactions on Automatic Control, Vol.AC-29, No.12, 1984.

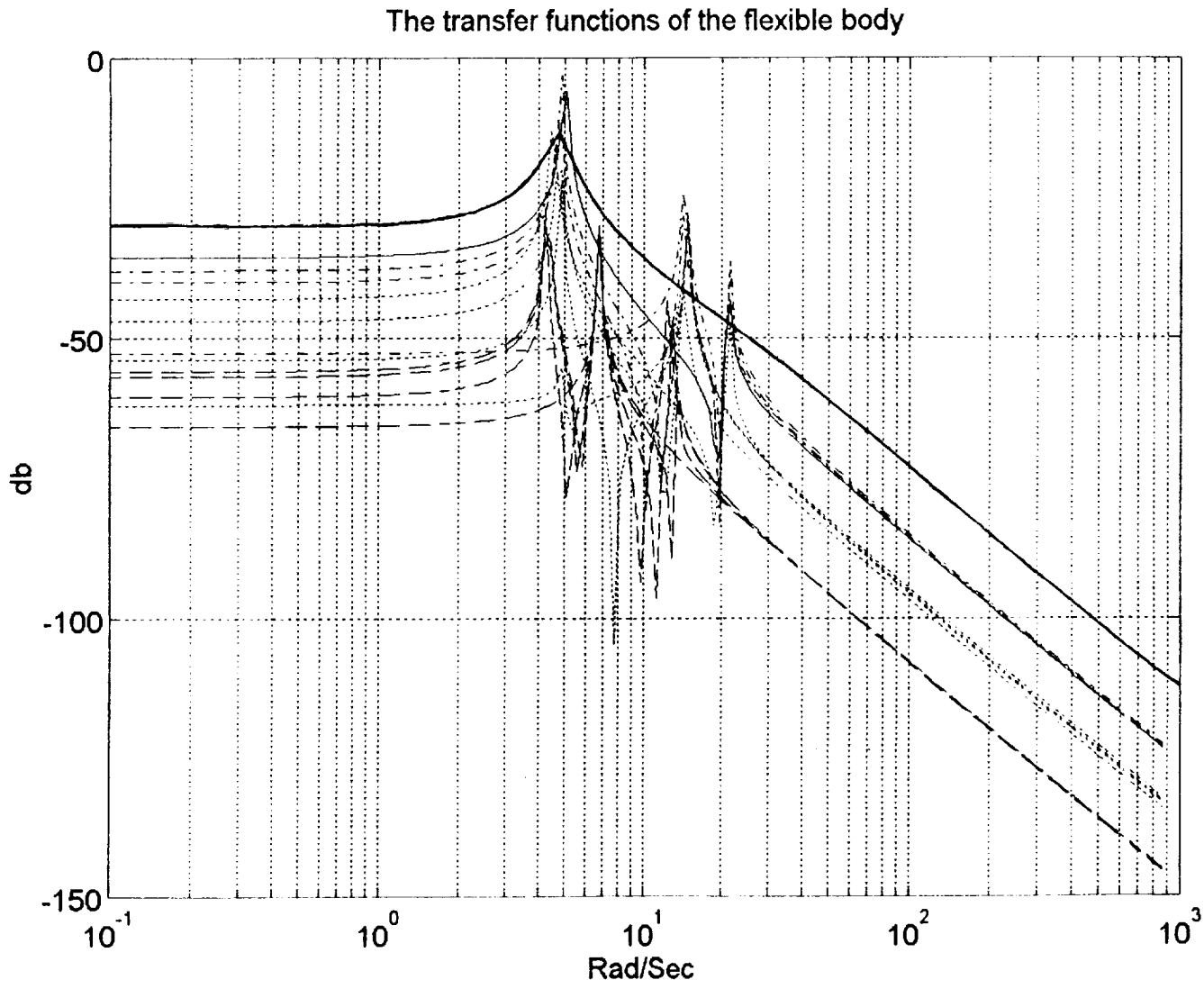

Fig. 4 The transfer functions of the flexible body (3 axes, 4 directions) with fixed natural frequencies.

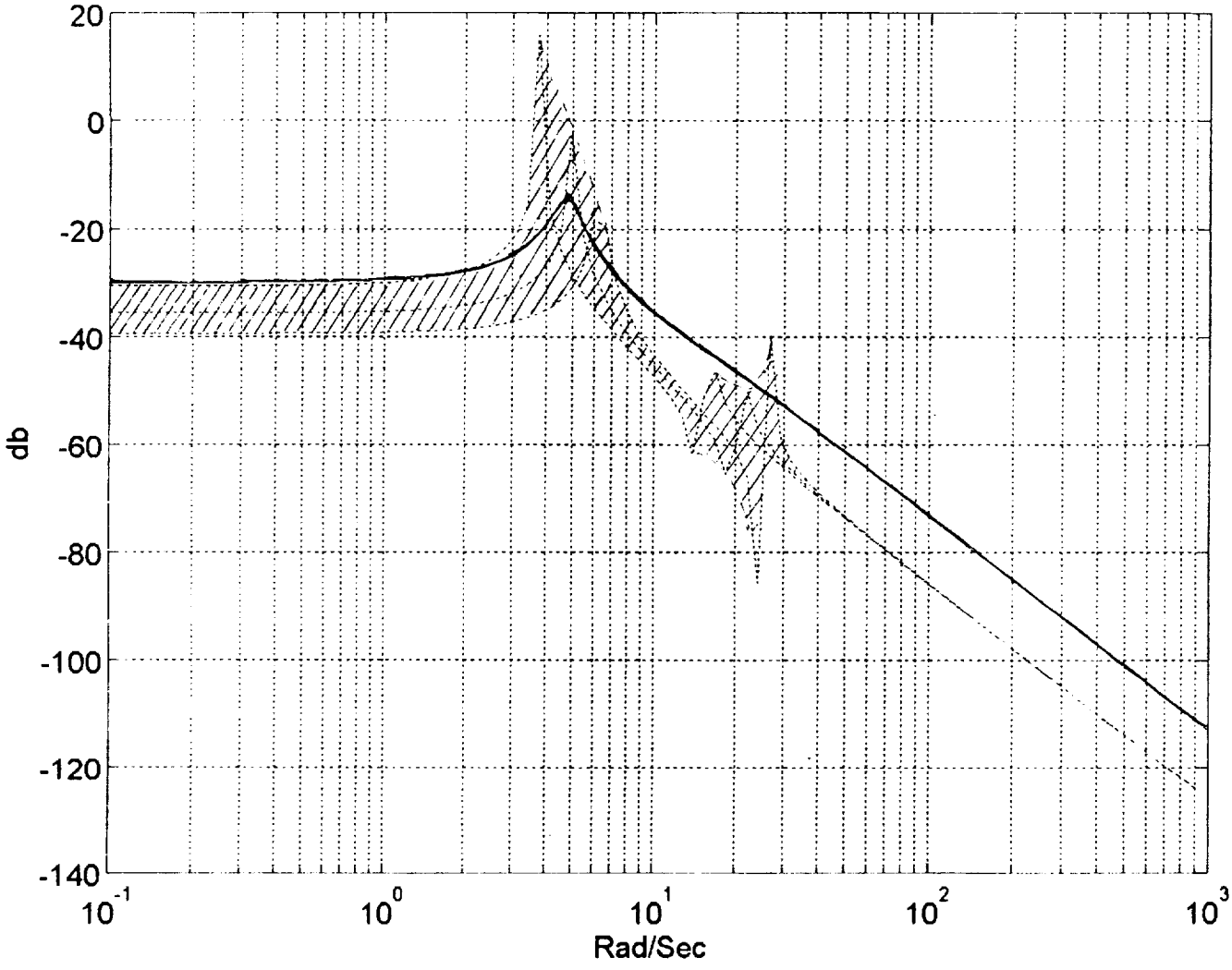

Fig. 5 Approximate maximum additive perturbation of the flexible body.

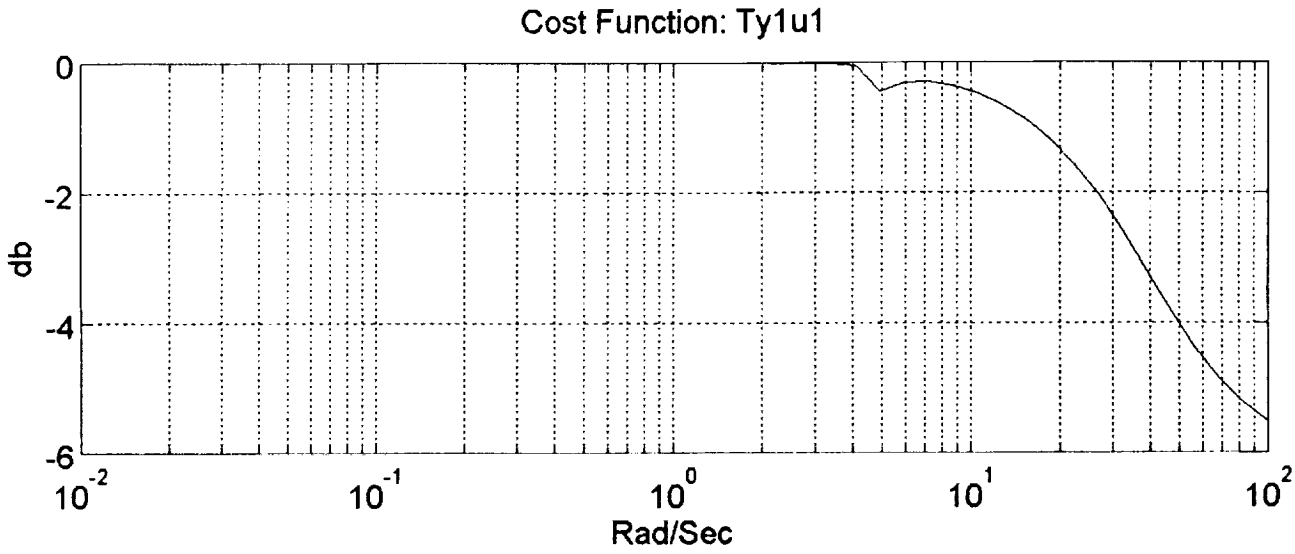

Fig. 6 The infinity norm of the closed-loop transfer function.

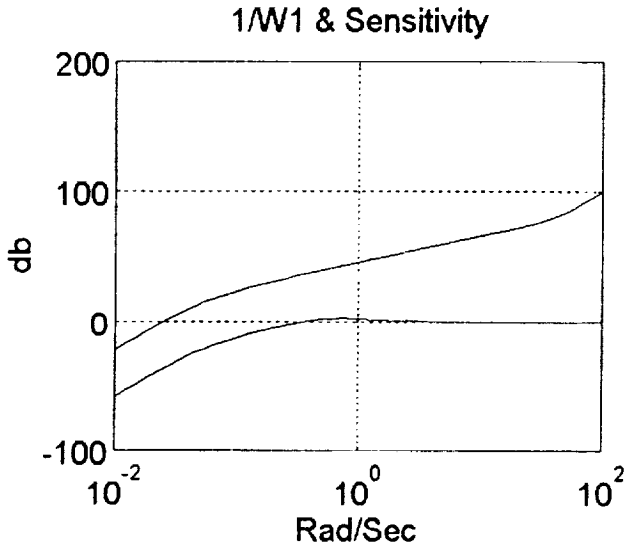

Fig. 7 W^{-1}_1 weighting and sensitivity function.

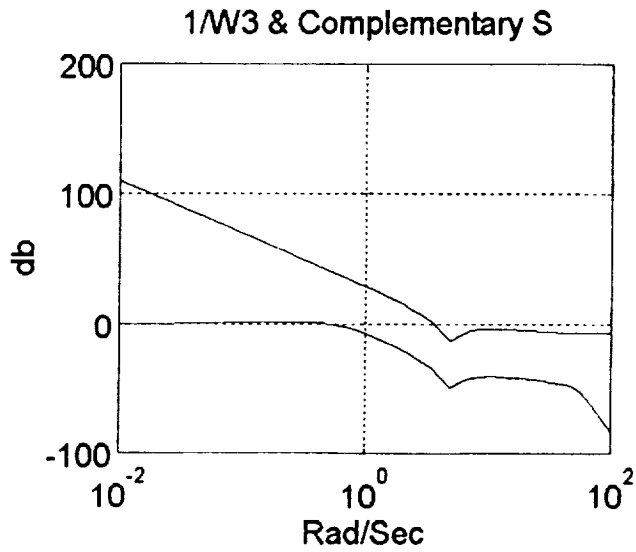

Fig. 8 W^{-1}_3 weighting and complementary sensitivity function.

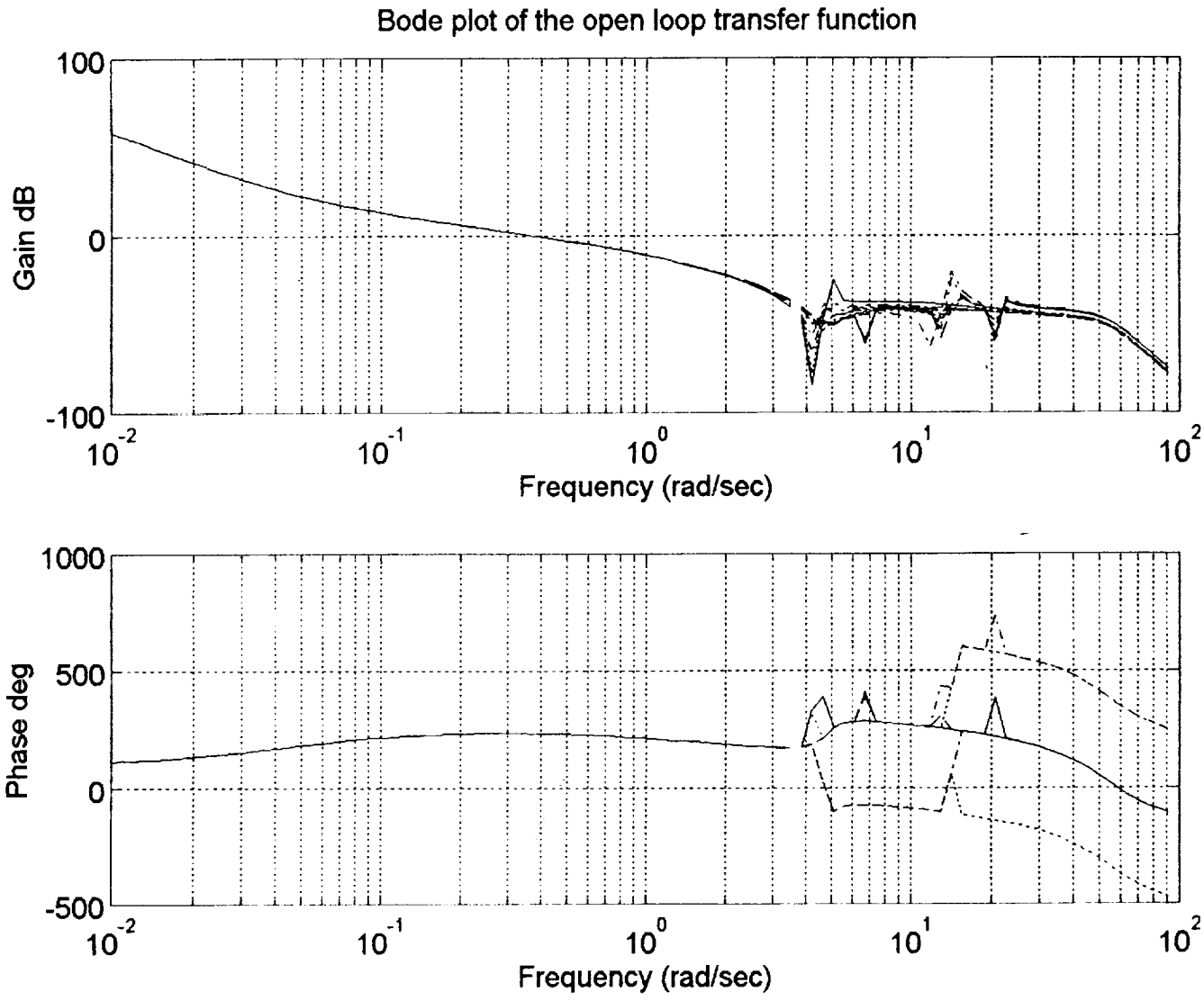

Fig. 9 The open loop transfer functions of the system (3 axes, 4 directions) with fixed the varities of the natural frequencies.

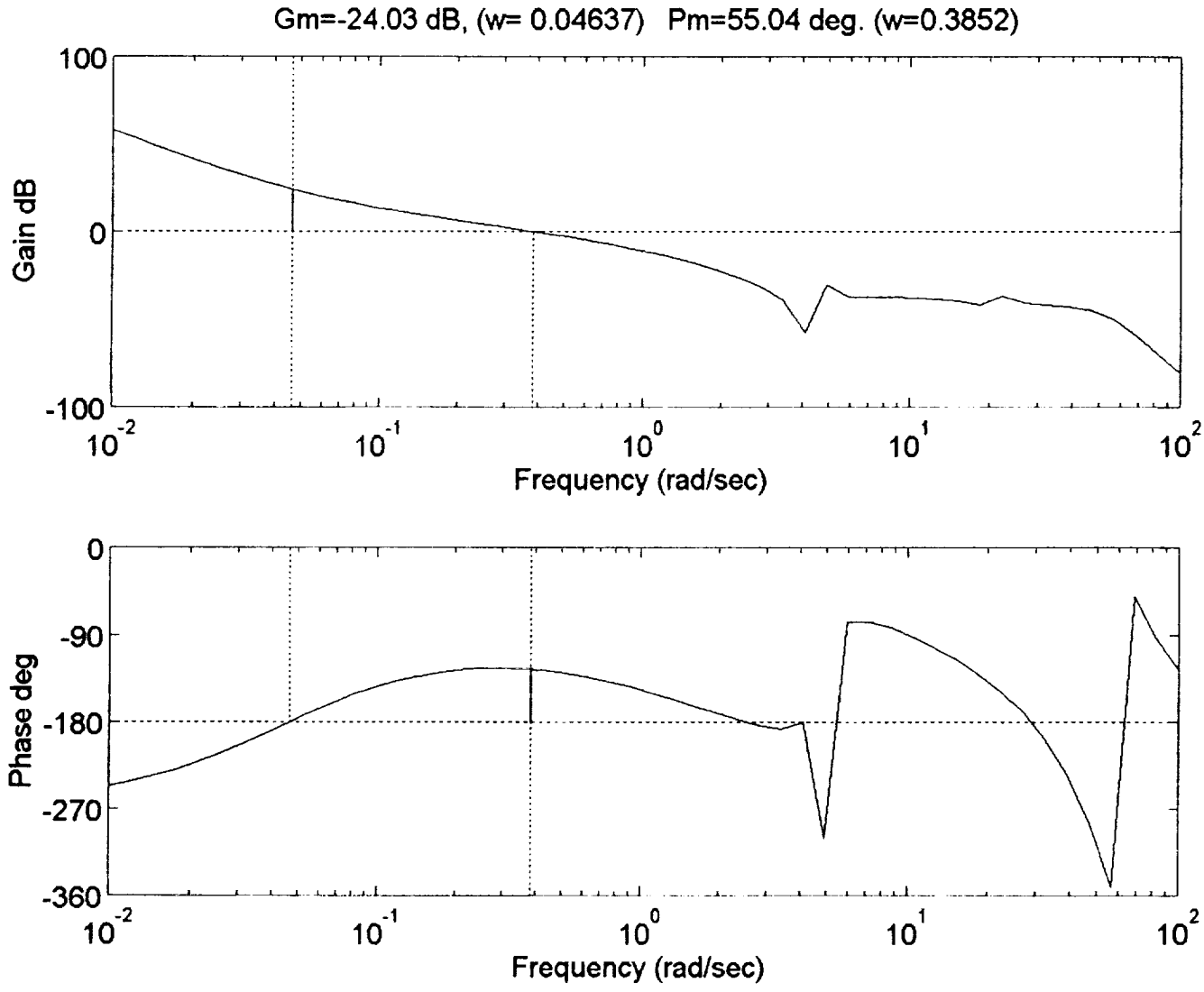

Fig. 10 Gain margin G_m and phase margin P_m of the system.

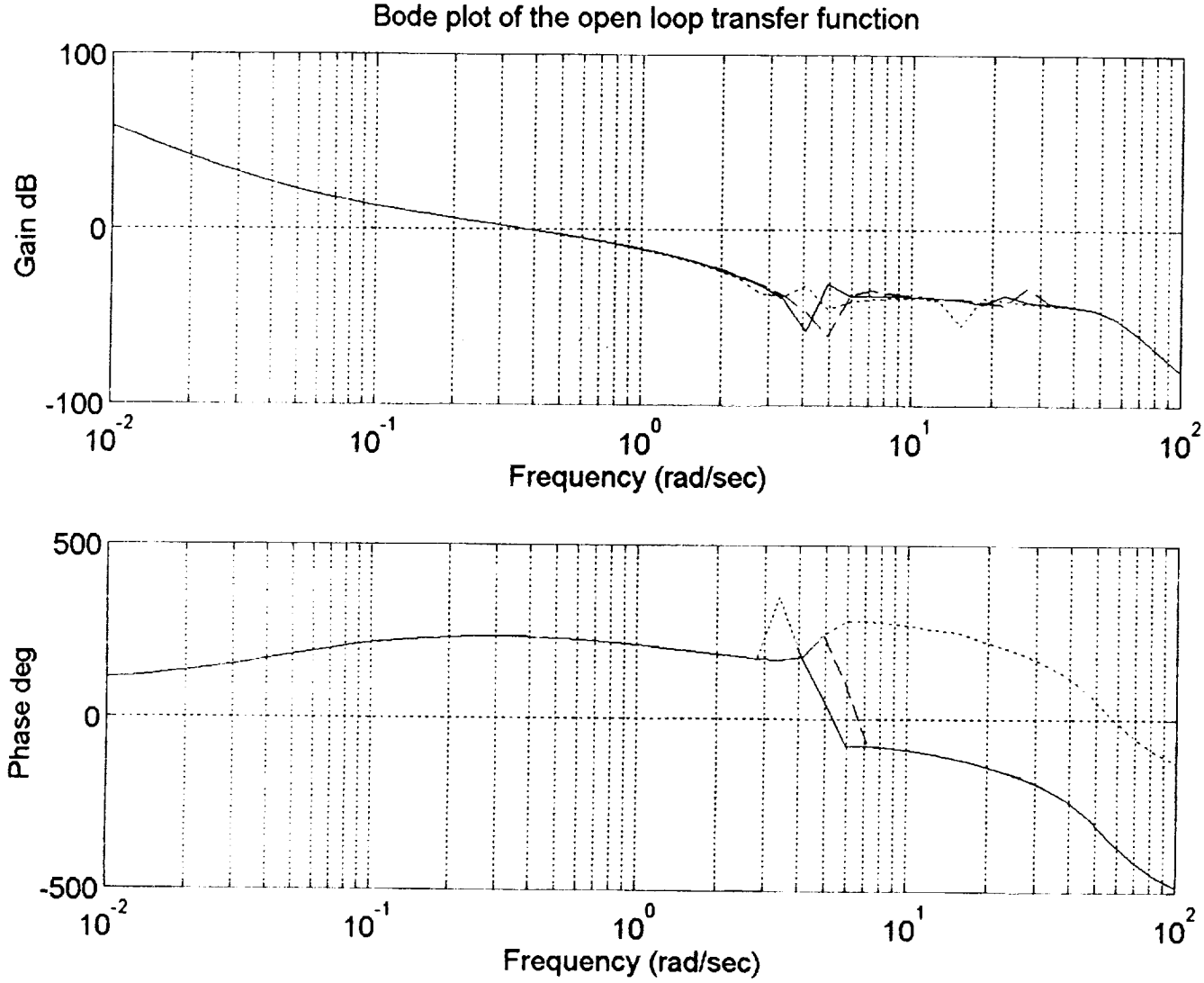

Fig. 11 The open loop transfer functions of the system (Z axis, β = 0 deg.) with varying natural frequencies from -25% to 25%.

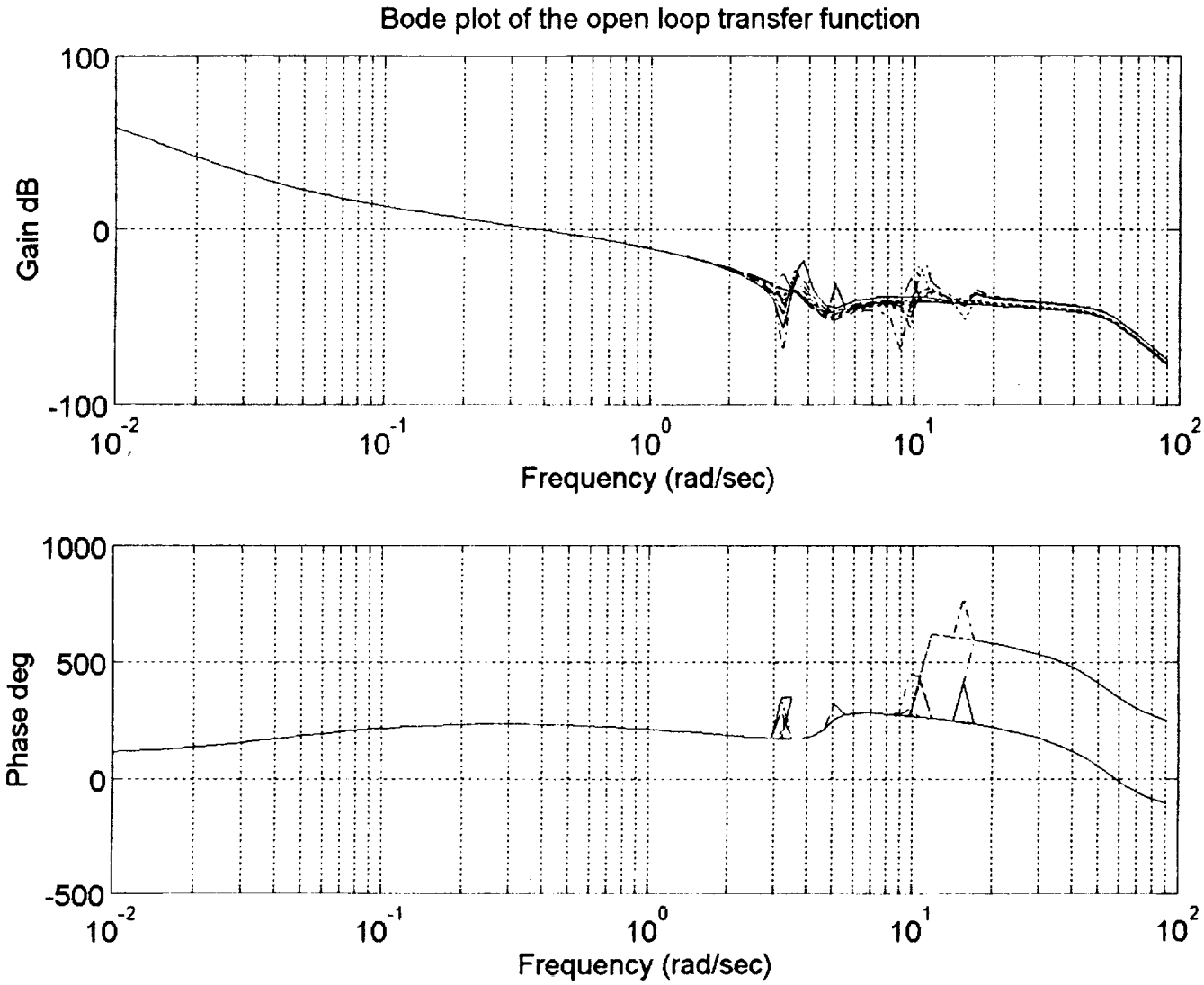

Fig. 12 The open loop transfer functions of the system (3 axes, 4 directions) with varying natural frequencies to -25%.

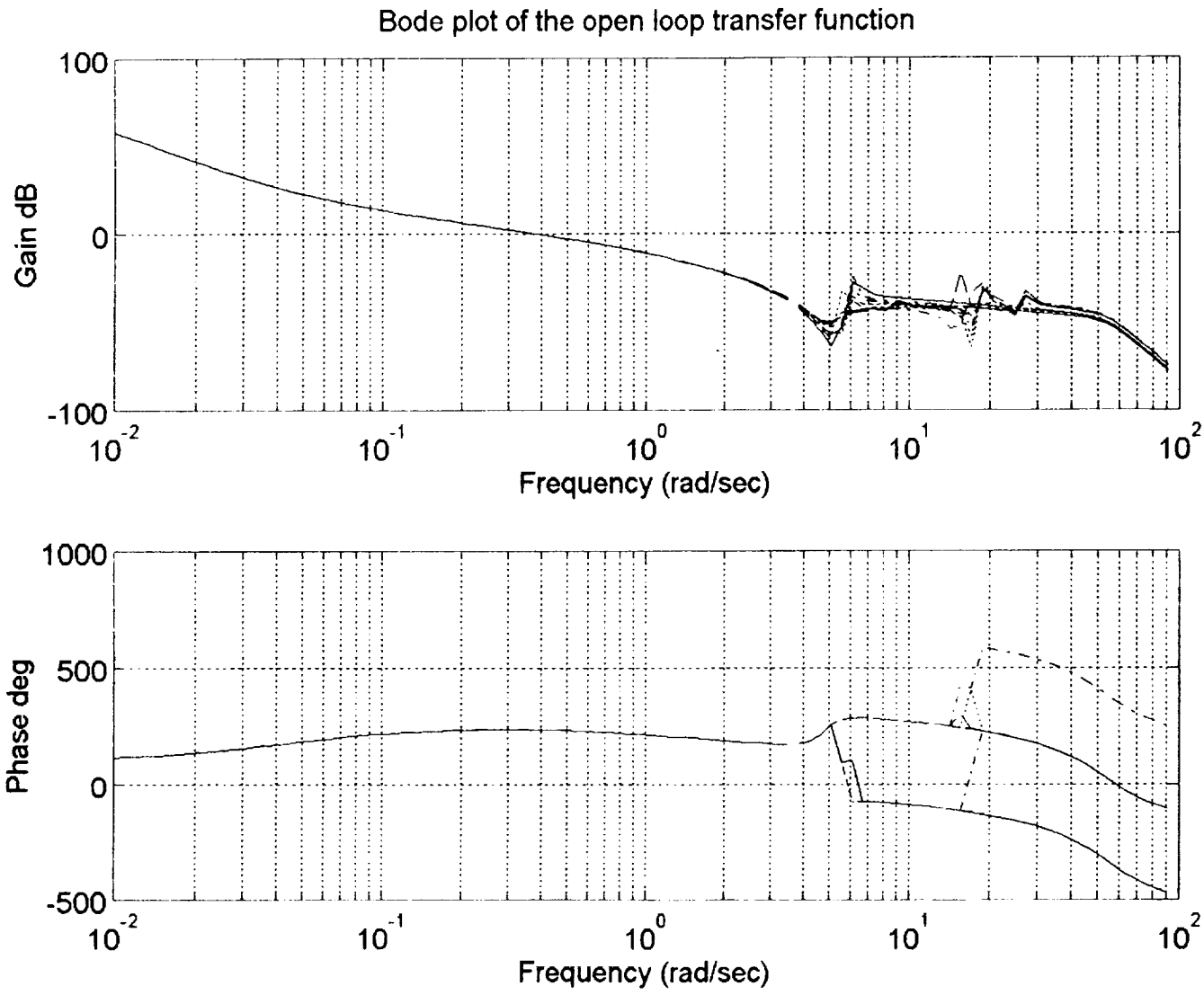

Fig. 13 The open loop transfer functions of the system (3 axes, 4 directions) with varying natural frequencies to 25%.

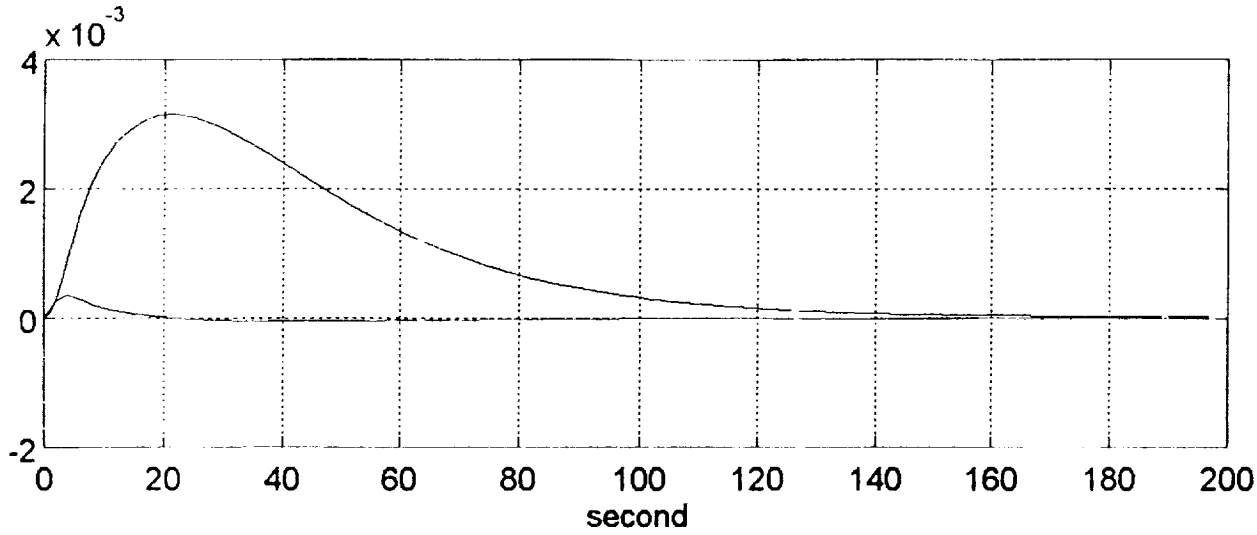

Fig. 14 Unit step response and unit impulse response (X axis, β = 0 deg.)

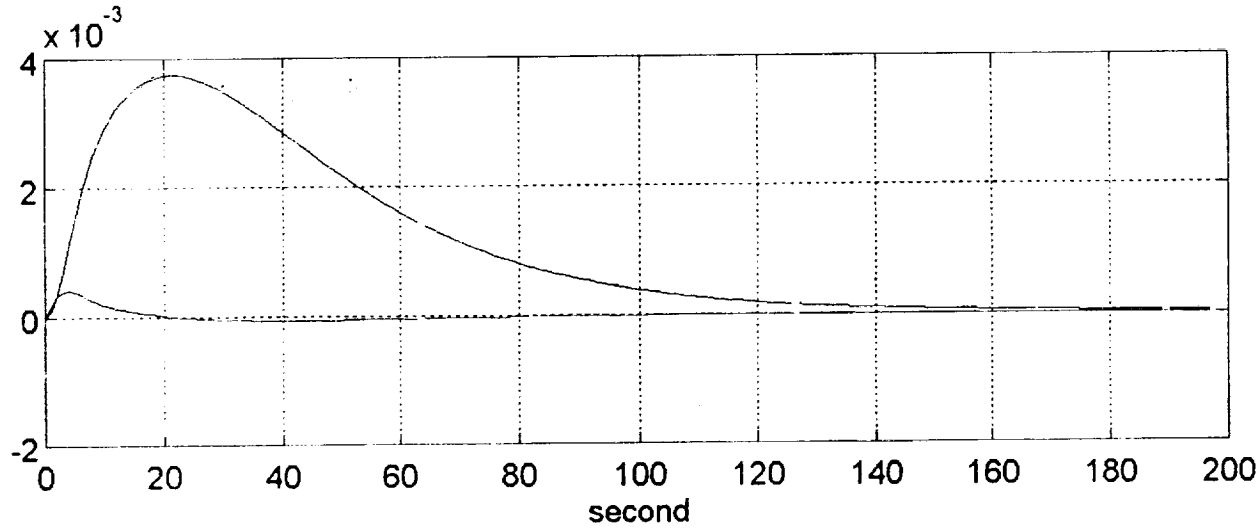

Fig. 15 Unit step response and unit impulse response (Y axis, β = 0 deg.)

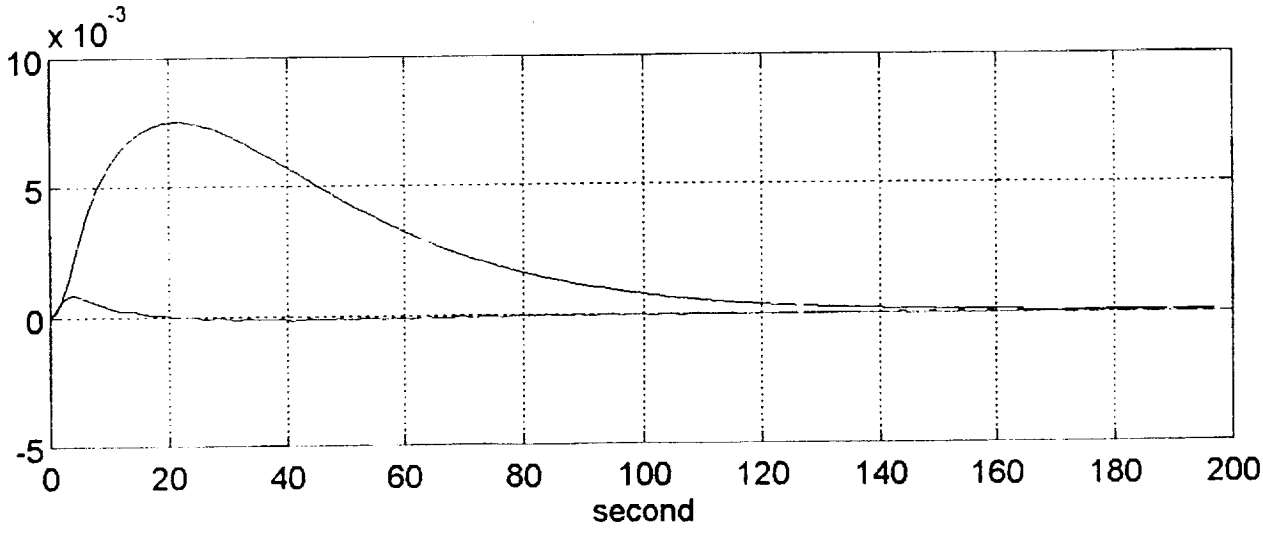

Fig. 16 Unit step response and unit impulse response (Z axis, β = 0 deg.)

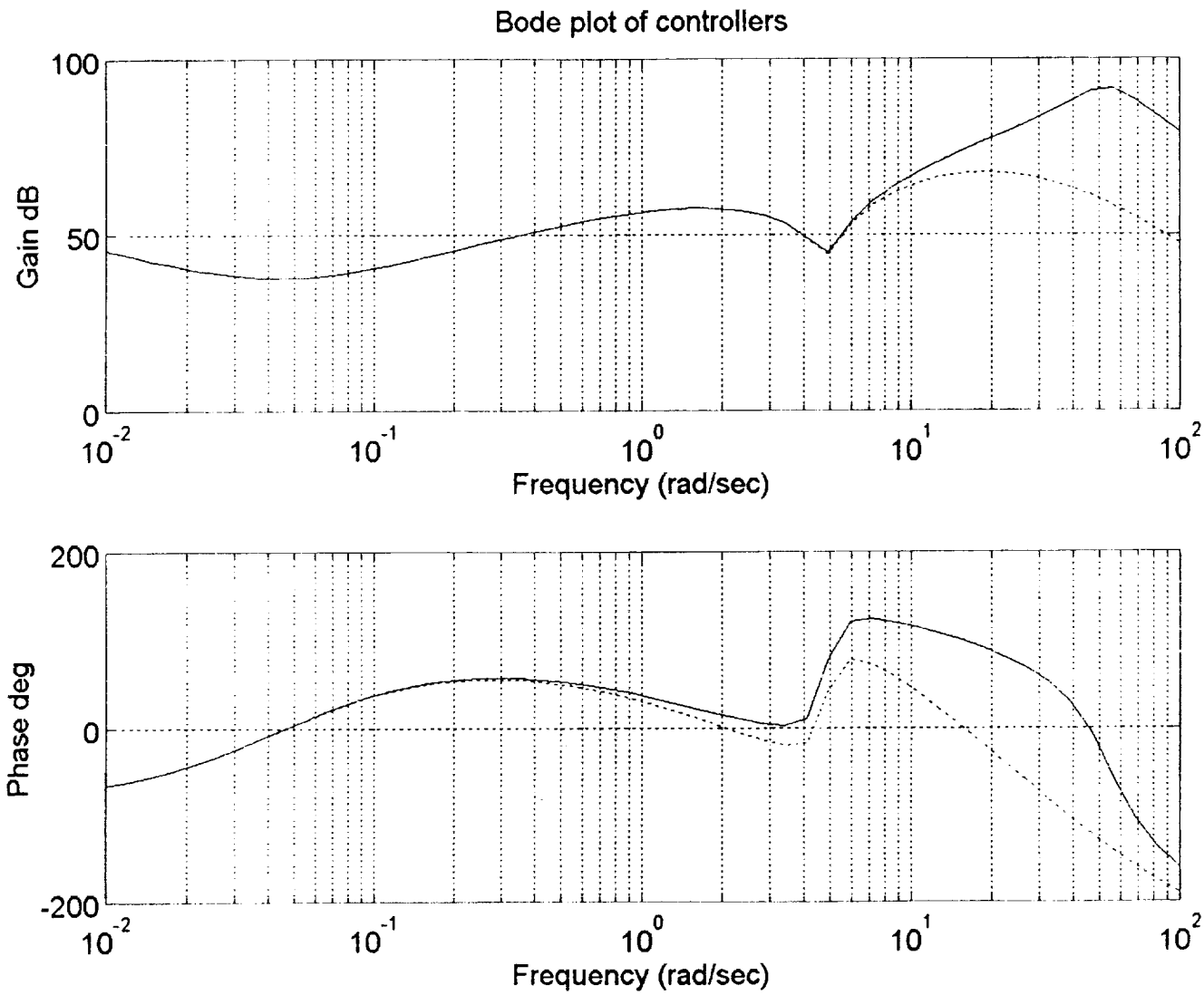

Fig. 17 The bode plots of the original and the fourth order reduced controllers (Z axis, β = 0 deg.)

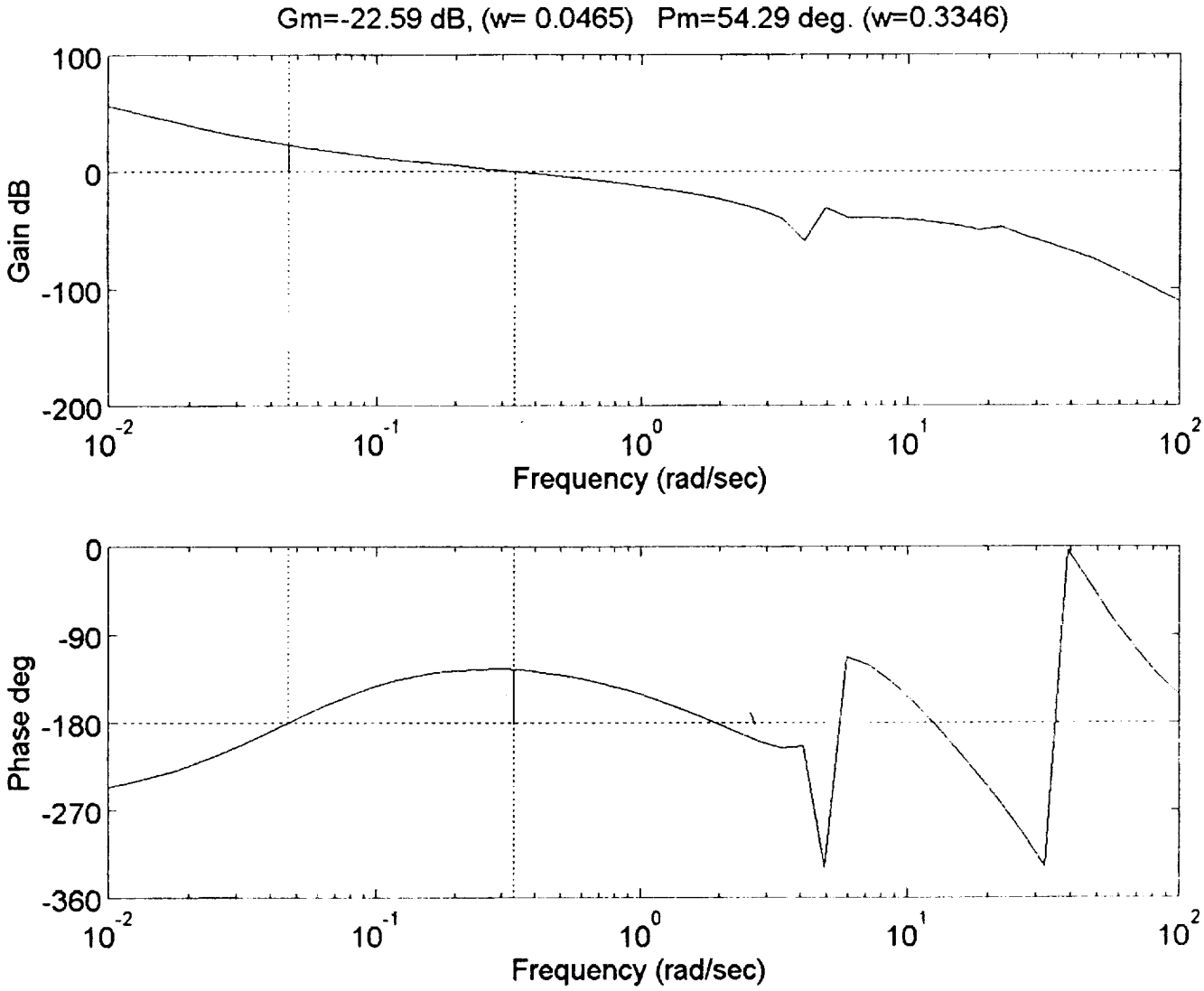

Fig. 18 Gain margin G_m and phase margin P_m of the system with the fourth order reduced controller (Z axis, β = 0 deg.)

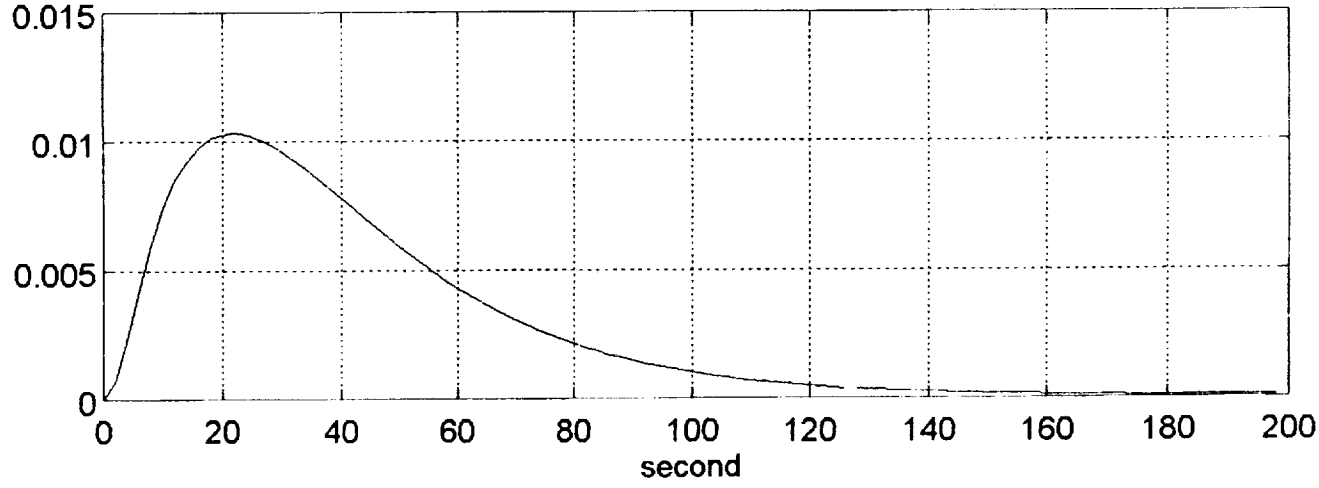

Fig. 19 Unit step response of the system with the fourth order reduced controller (Z axis, β = 0 deg.)

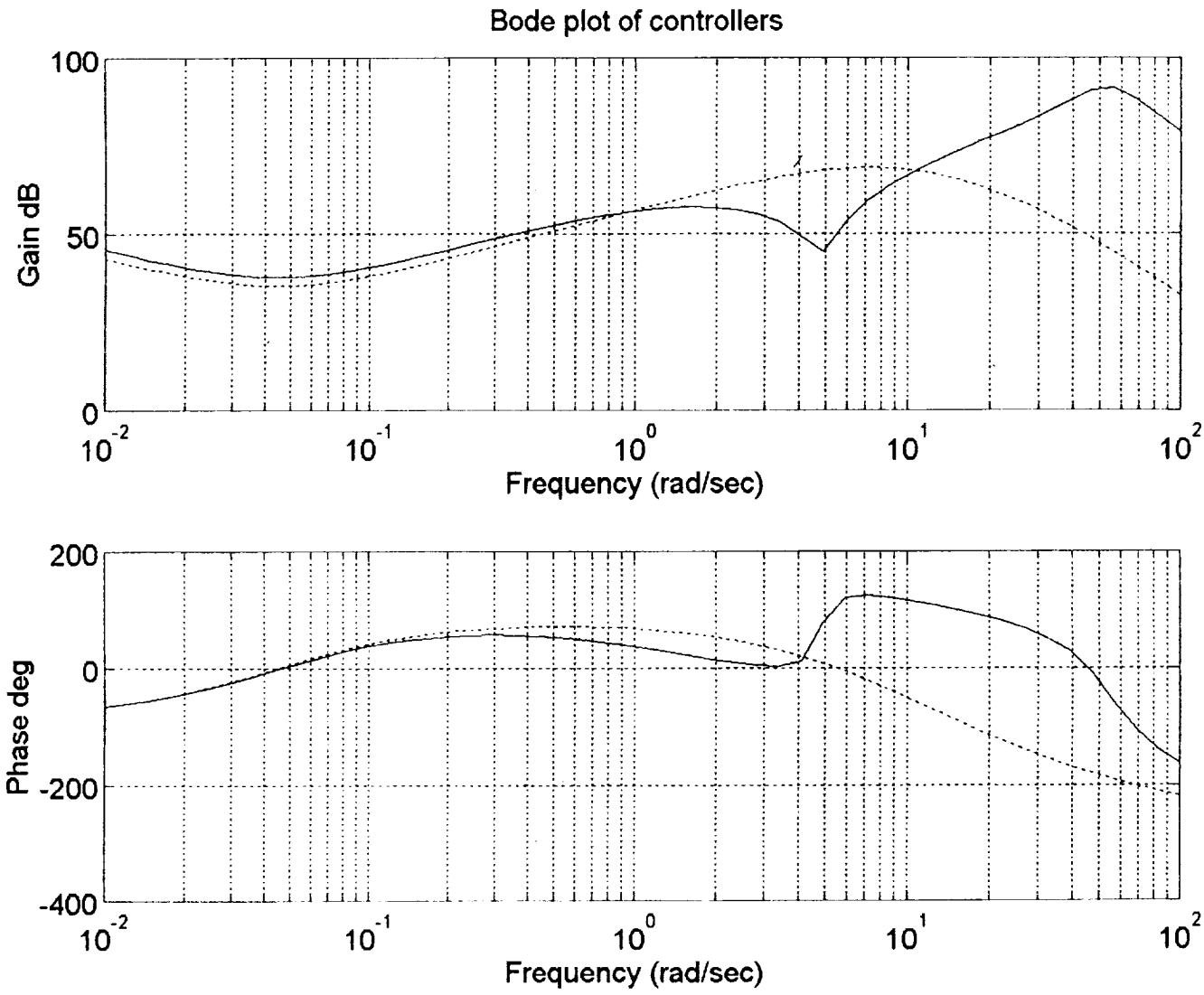

Fig. 20 The bode plots of the original and the second order reduced controllers (Z axis, β = 0 deg.)

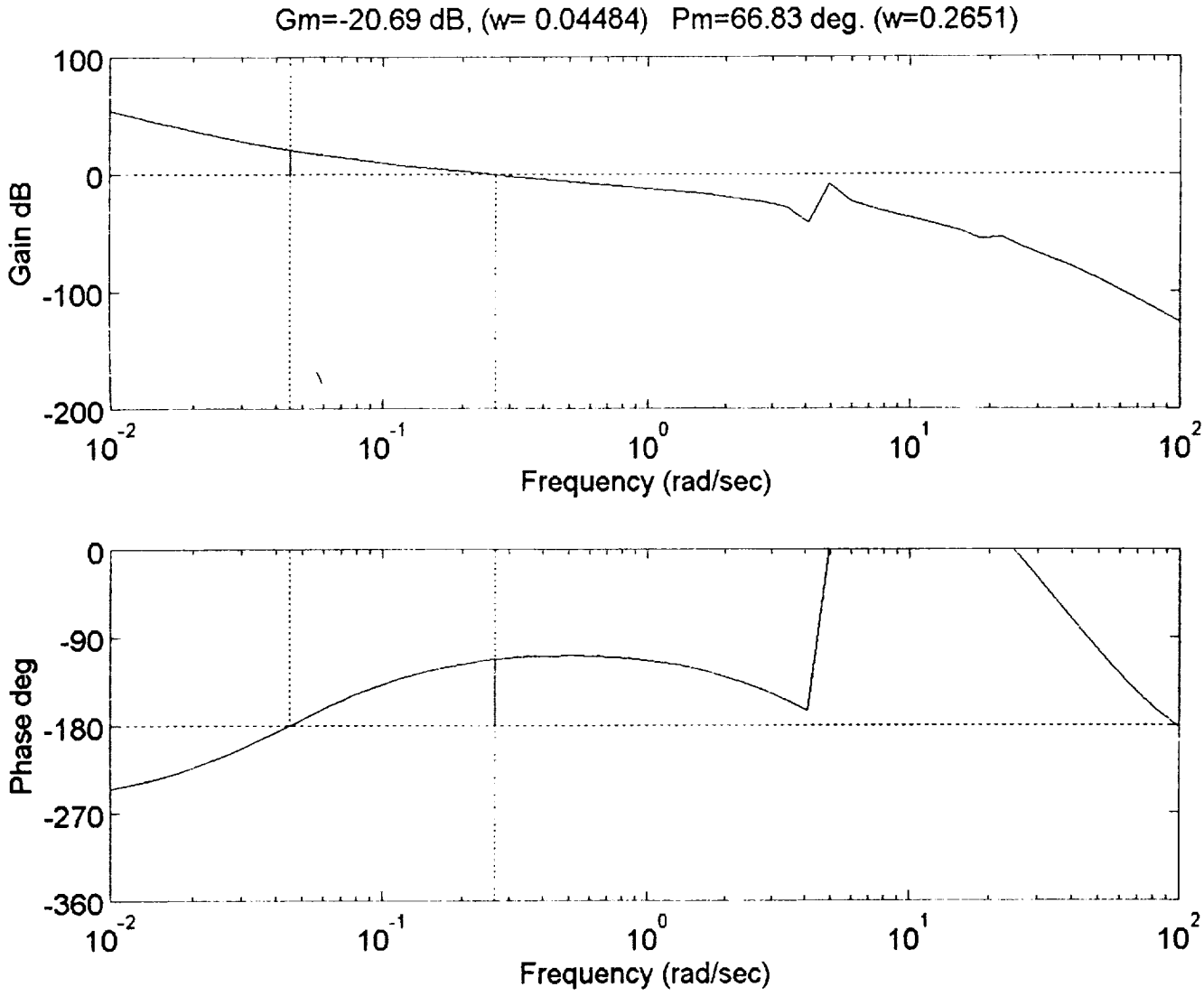

Fig. 21 Gain margin G_m and phase margin P_m of the system with the second order reduced controller (Z axis, β = 0 deg.)

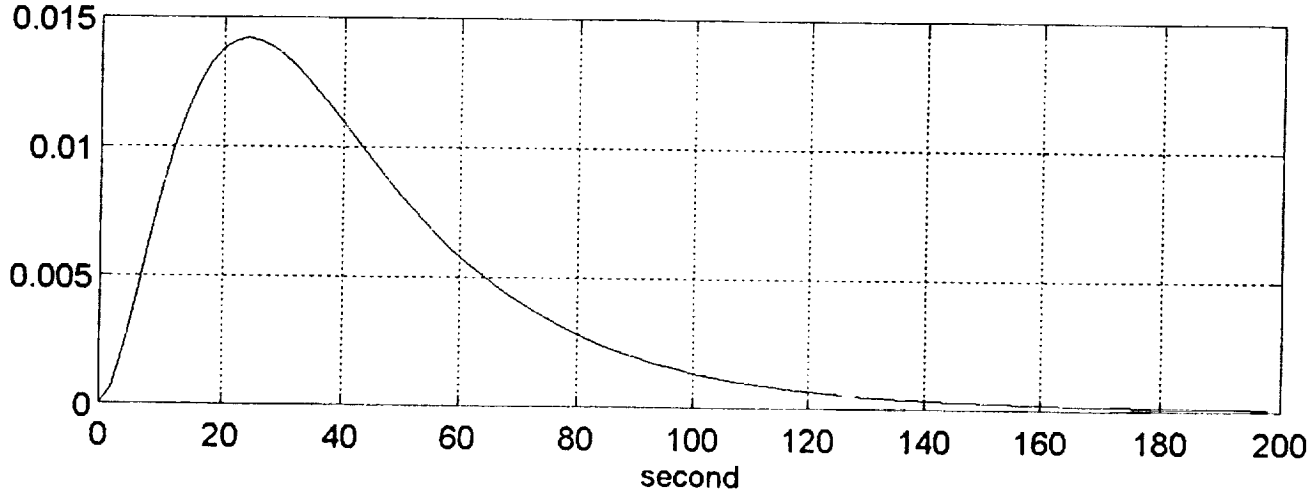

Fig. 22 Unit step response of the system with the second order reduced controller (Z axis, β = 0 deg.)

$$F(Q^4) = \bigcup_{i=1}^{C_4^2 2^{4-2}} F(f_i^2)$$

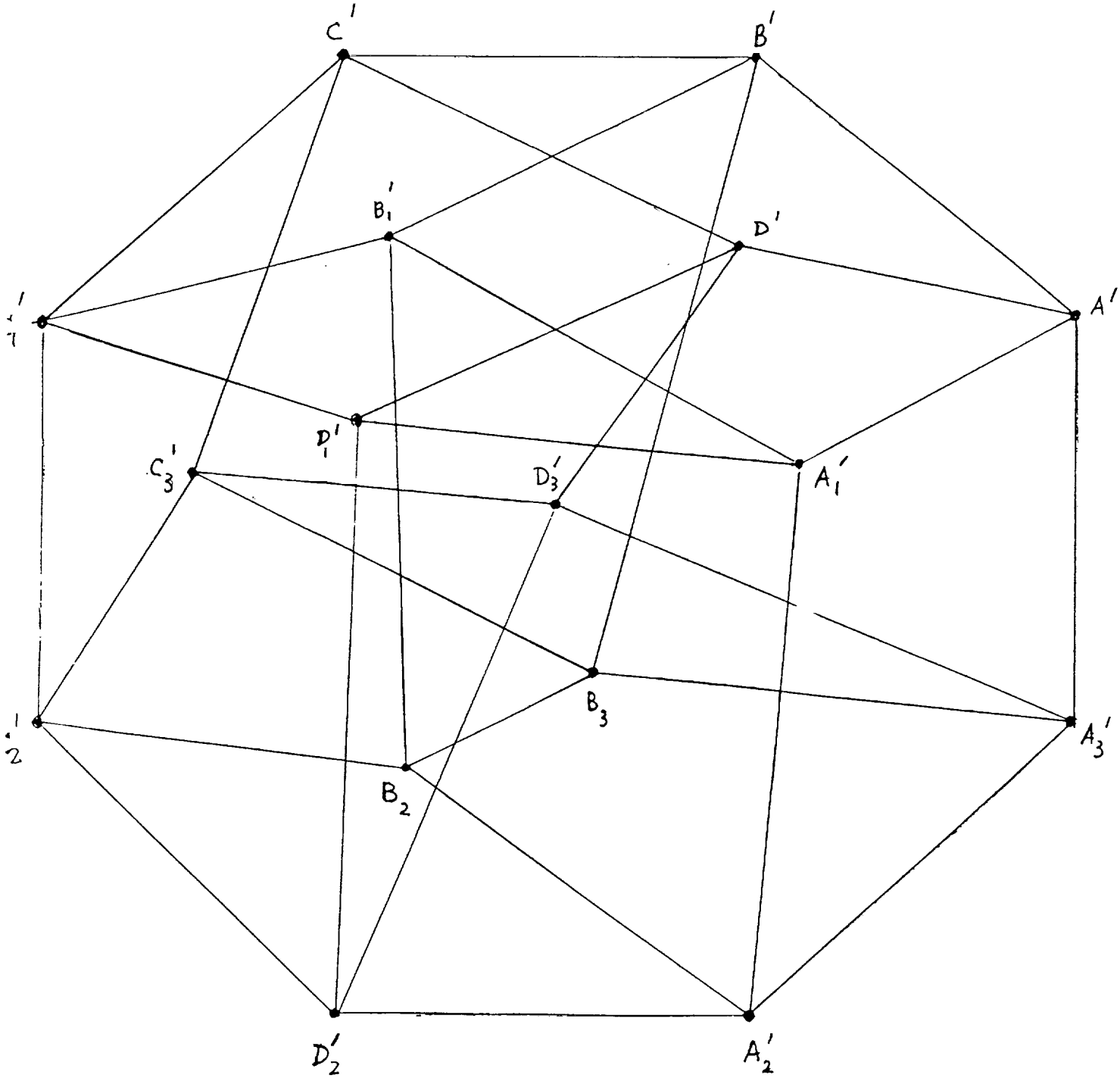

Image of Q in 4-Dimensional space

02/23/94 11:23 AM

Face Theorem for R^3

If F *is a holomorphic function in* C *whose real part and imaginary part are affine, multilinear functions of* $Q \subset R^3$ *and* f_i , i=1,. .,6 , *are the two-dimensional, exposed faces of* Q, *then* $\bigcup_{i=1}^{6} F(f_i) = \text{Im}\{F(Q)\}$

Proof:

It is obvious that $\bigcup_{i=1}^{6} F(f_i) \subseteq \text{Im}\{F(Q)\}$.

Suppose $\exists\ p' \in \text{Im}\{F(Q)\} \ni p' \notin F(f_i)\ \forall\ i$. Since $p' \in \text{Im}\{F(Q)\}\ \exists$ some $q' \in Q \ni p' = F(q')$. Furthermore, q' is an interior point of Q so that $\exists$ a line segment l in $Q \ni l$ passes through q', l is parallel to the axes, and the endpoints q_t and q_b of l lie on faces f_t and f_b , respectively, of Q. Since F is multilinear, $F(l)$ is a line segment in $\text{Im}\{F(Q)\}$.

Consider any neighborhood of q_t, $N_t = \{q \in f_t \mid d(q,q_t) < \varepsilon_0\}$. Since F is continuous $F(N_t) \subset F(f_t)$ and $F(N_t) = N_0$ is a neighborhood of $F(q_t)$. Choose any point $p_1 \in N_0$ such that p_1 is distinct from $F(q_t)$ and $p_1 \in F(l)$. Choose a neighborhood of p_1, $N_1 = \{F(q) \in F(Q) \mid d(q,q_1) < \varepsilon_1 , F(q_1) = p_1, q_1 \in l\}$. Continue this process, choosing p_i from the neighborhood $N_{i-1} \cap F(l)$, such that p_i is distinct from p_{i-1}, and $\ni d(q_i,q_t) > d(q_{i-1},q_t)$. For each p_i , choose a neighborhood of p_i, $N_i = \{F(q) \in F(Q) \mid d(q,q_i) < \varepsilon_i , F(q_i) = p_i , q_i \in l\}$. Without loss of generality, assume that there are a finite number, κ of such neighborhoods generated and that $p_\kappa = F(q_b)$.

$F(l)$ is completely covered by the union of these neighborhoods and $\exists$ some $i = k_1 \ni N_{k_1}$ contains points of the interior of $F(f_t)$, points from $\partial\{F(f_t)\}$ and points in F(Q) but not in $F(f_t)$. There also exists some $i = m_1 \ni N_{m_1}$ contains points from $F(\partial\{f_t\})$ and points in $F(f_t)$ where $k_1 \geq m_1$. The preimage of each N_i, i = 0, ..., k_1, intersects f_t. In particular, the set $\left[\bigcup_{i=m_1}^{k_1} N_i\right] \cap F(l)$ is a line segment in F(Q). Since F is multilinear, the preimage of this set contains a line segment that is parallel to the axes. This line segment is in Q and intersects f_t only at an edge so that it must lie on some face, f_{k_1}, of Q, $k_1 \neq t$.

Consider all neighborhoods N_i, $i > k_1$, $\ni N_i \cap F(f_{k_1}) \neq \varnothing$. One of these neighborhoods, N_{k_2}, contains points from the interior of $F(f_{k_1})$, points from $\partial\{F(f_1)\}$ and points in F(Q) but not in $F(f_1)$. There also exists some $i = m_2 \ni N_{m_2}$ contains points from $F(\partial\{f_1\})$ and points in $F(f_1)$ where $k_2 \geq m_2$. The preimage of each N_i, $i = k_1, \ldots, k_2$, intersects f_1. In particular, the set $\left[\bigcup_{i=m_2}^{k_2} N_i\right] \cap F(l)$ is a line segment in F(Q).

Since F is multilinear, the preimage of this set contains a line segment that is parallel to the axes. This line segment is in Q and intersects f_1 only at an edge so that it must lie on some face, f_{k_2}, of Q, $k_2 \neq k_1$

Since there are a finite number of neighborhoods, this process can be continued until we reach the point p_K and its neighborhod N_K so that all points on l lie on some face of Q. Since $p' \in l$ then p' must lie on some face of Q which contradicts the assumption that $p' \notin F(f_i) \ \forall\, i$. Thus $\mathrm{Im}\{F(Q)\} \subseteq \bigcup_{i=1}^{6} F(f_i)$

$\therefore \bigcup_{i=1}^{6} F(f_i) = \mathrm{Im}\{F(Q)\}$

Face Theorem for R^n

If F *is a holomorphic function in* C *whose real part and imaginary part are affine, multilinear functions of* $Q \subset R^n$ *and* f_i, i=1,...,m *are the two-dimensional, exposed faces of* Q *with* $m = C_n^2 2^{n-2}$ *then* $\bigcup_{i=1}^{m} F(f_i) = \mathrm{Im}\{F(Q)\}$

The proof of this theorem follows from the three-dimensional case by considering each of the two-dimensional exposed faces of $Q \subset R^n$, fixing all but two of the dimensions of Q at a time and applying the method used in the proof above.